Estimation of energy expenditure during treadmill exercise via thermal imaging

Jensen, Martin Møller; Poulsen, Mathias Krogh; Alldieck, Thiemo; Larsen, Ryan Godsk; Gade, Rikke; Moeslund, Thomas B.; Franch, Jesper

Published in:
Medicine and Science in Sports and Exercise

DOI (link to publication from Publisher):
10.1249/MSS.0000000000001013

Publication date:
2016

Document Version
Accepted author manuscript, peer reviewed version

Medicine & Science IN Sports & Exercise
The Official Journal of the American College of Sports Medicine
www.acsm-msse.org

. . . Published ahead of Print

Estimation of Energy Expenditure during Treadmill Exercise via Thermal Imaging

MARTIN MØLLER JENSEN[1], MATHIAS KROGH POULSEN[2], THIEMO ALLDIECK[1], RYAN GODSK LARSEN[2], RIKKE GADE[1], THOMAS BALTZER MOESLUND[1], and JESPER FRANCH[2]

[1]Department of Architecture, Design and Media Technology, Aalborg University, Aalborg, Denmark; [2]Department of Health Science and Technology, SMI, Aalborg University, Aalborg, Denmark

Accepted for Publication: 6 June 2016

Medicine & Science in Sports & Exercise, Publish Ahead of Print
DOI: 10.1249/MSS.0000000000001013

Estimation of Energy Expenditure during Treadmill Exercise via Thermal Imaging

MARTIN MØLLER JENSEN[1], MATHIAS KROGH POULSEN[2], THIEMO ALLDIECK[1], RYAN GODSK LARSEN[2], RIKKE GADE[1], THOMAS BALTZER MOESLUND[1], and JESPER FRANCH[2]

[1]Department of Architecture, Design and Media Technology, Aalborg University, Aalborg, Denmark; [2]Department of Health Science and Technology, SMI, Aalborg University, Aalborg, Denmark

Corresponding author: Jesper Franch
Department of Health Science and Technology, SMI
Aalborg University
DK 9220 Aalborg Ø
Denmark
jfranch@hst.aau.dk

The authors declare no conflicts of interest, financial or otherwise. The results of the present study do not constitute endorsement by the American College of Sports Medicine.

ABSTRACT

Purpose: Non-invasive imaging of oxygen uptake may provide a useful tool for quantification of energy expenditure during human locomotion. A novel thermal imaging method (optical flow) was validated against indirect calorimetry for estimation of energy expenditure during human walking and running. **Methods:** Fourteen endurance-trained subjects completed a discontinuous incremental exercise test on a treadmill. Subjects performed 4-min intervals at 3, 5 and 7 km $\cdot hr^{-1}$ (walking) and at 8, 10, 12, 14, 16 and 18 km $\cdot$ hr^{-1} (running) with 30 s of rest between intervals. Heart rate, gas exchange and mean accelerations of ankle, thigh, wrist and hip were measured throughout the exercise test. A thermal camera (30 frames $\cdot$ s^{-1}) was used to quantify optical flow, calculated as the movements of the limbs relative to the trunk (internal mechanical work), and vertical movement of the trunk (external vertical mechanical work). **Results:** Heart rate, gross oxygen uptake (mL $\cdot$ kg^{-1} $\cdot$ min^{-1}) together with gross and net energy expenditure (J $\cdot$ kg^{-1} $\cdot$ min^{-1}) rose with increasing treadmill velocities, as did optical flow measurements and mean accelerations (g) of ankle, thigh, wrist and hip. Oxygen uptake was linearly correlated with optical flow across all exercise intensities (R^2 = 0.96, P<0.0001; VO_2 (mL $\cdot$ kg^{-1} $\cdot$ min^{-1}) = 7.35 + 9.85 × optical flow (arb. units)). Only 3-4 s of camera recording were required to estimate an optical flow value at each velocity. **Conclusions:** Optical flow measurements provide an accurate estimation of energy expenditure during horizontal walking and running. The technique offers a novel experimental method of estimating energy expenditure during human locomotion, without use of interfering equipment attached to the subject.

Key Words: Oxygen Uptake, Walking, Running, Accelerometry, Thermal Optical Flow

INTRODUCTION

Direct and accurate quantification of energy expenditure (EE) during human movement can be obtained through oxygen uptake measurements. Early investigations of oxygen uptake during exercise were performed using the Douglas bag method (1, 21, 37) and more recently metabolic carts have been validated and used for measurements of oxygen uptake (7, 10). However, the equipment necessary to quantify oxygen uptake may interfere with the normal locomotive pattern of the subject.

Indirect quantification of EE during exercise typically involves heart rate monitors (12), accelerometers (12), and GPS (22) or combinations of these devices (3, 12), which have been validated against oxygen uptake (12). In most cases heart rate monitors requires attachment of a chest strap and a wristwatch for data collection. Heart rate measurements may introduce inaccuracy because emotional stress, environmental stress (i.e. cold, heat and altitude exposure) and training status can affect the association between oxygen uptake and heart rate, especially at low exercise intensities (12, 30, 32).

Accelerometers are used to quantify accelerations of the body and are widely used to quantify EE during activities of daily living (for review see ref. 29). Quantification is normally achieved with an accelerometer positioned close to the body's center of mass (i.e. hip or lower back). However, accelerometers have some well-known limitations. Uniaxial accelerometer counts have been shown to predict oxygen uptake during walking (4, 12) but accelerometer counts does not change significantly with increased speed during slow and fast running (4, 12). Precision can be improved further by using triaxial accelerometers (12). With uniaxial accelerometers positioned at the ankle, counts are higher compared with hip placed accelerometers (15). This

indicates that acceleration counts from body segments involved in running locomotion will reflect change in speed of locomotion, and therefore provide a valid registration of energy expenditure during walking and running.

So far, both direct (oxygen uptake) and indirect (heart rate registration, accelerometry, GPS) quantification of EE during walking and running requires equipment attached directly to the person disposed for examination. Furthermore, oxygen uptake- and heart rate measurements normally require 2-3 min of data collection before valid steady state measurements can be obtained. Therefore, a fast method of measuring EE would be relevant for estimating EE in many sports activities involving walking and running.

Within the field of computer vision, human motion analysis aim to track and detect people as well as interpret their motions (36, 39). Motion interpretation can be used within medical diagnosis, public health and sports analysis. Lately, thermal imaging has been introduced as a relevant method for quantification of movement (14). Thermal cameras are applied in this field for two reasons. Firstly, thermal cameras measure the amount of thermal radiation of objects in a scene. As long as the temperature of the person is different from the environment, a thermal camera is a valid tool to detect and track people, because the background separation is almost given by the input data. Absolute and relative temperature changes as such are therefore not quantified by the method. Secondly the identities of individuals are hidden in thermal data and hence open up a range of applications in public areas without violating any privacy issues. Furthermore, thermal cameras are relatively inexpensive to purchase and data collection requires no interfering equipment attached to the subject during test.

Optical Flow is defined as the movement of entities in succeeding images (23). As long as the movements take place in a plane parallel to the image plane in the camera, the optical flow is a direct measure of movement. Thermal optical flow is defined as optical flow estimated in succeeding thermal images (33). The different algorithms behind optical flow are all based on an assumption that an image entity has the same appearance in two consecutive images. This assumption is often violated and different optimization methods are therefore used (6).

The acceleration and lift of a person's centre of mass is defined as external mechanical work (8) and referred to as global movement in digital analysis, whereas movement of the limbs relative to the person's trunk is defined as internal mechanical work (8)and referred to as local movement. The total amount of local movement is used in this investigation as a measuring system for motion of body segments (i.e. arm and leg movement) in relation to the torso. Dynamic high intensity exercise such as fast running require fast motion of body limbs, while low energy consuming motions require fewer and slower movements of arms and legs. Early work has described methods to determine if a person is walking or running by analyzing their cyclic motion pattern (13, 17). These previous studies mostly focus on labeling postures and activities while general descriptive methods about human motion or energy costs are lacking.

The aim of this project was therefore to validate a novel camera-based method for measuring EE during human locomotion without the use of any type of equipment hindering movements and performance. The camera-based method was validated against steady state oxygen uptake during horizontal walking and running. In addition, the time required to obtain valid estimations of EE through optical flow was examined. It was hypothesized that optical flow would demonstrate a strong linear relationship with oxygen uptake.

METHODS

Subjects: Thirteen male and one female subjects, age 28.1 ± 8.2 yr, weight 69.9 ± 7.5 kg, height 177.6 ± 7.8 cm, BMI 22.1 ± 1.7 kg $\cdot$ m^{-2} (mean ± SD) completed the study. All participants were recreational distance runners and had practiced distance and interval training for more than 2 yr. All subjects were fully informed of any risks associated with the study before giving their informed consent. The protocol was approved by the regional Ethics Committee (N-20140076).

Exercise testing. Exercise tests were performed on a motorized treadmill (Woodway Pro XL, Woodway Inc., Wisconsin, USA). All subjects were familiarized with treadmill running and had previously been involved in treadmill testing. Each exercise period was 4 min, separated by 30 sec rest. The duration of each exercise period was designed to elicit steady state oxygen consumption. Subjects covered three walking intervals at 3, 5 and 7 km $\cdot$ hr^{-1} and six running intervals at 8, 10, 12, 14, 16 and 18 km $\cdot$ hr^{-1}. Velocities increased from slowest to fastest as described by Fudge and co-workers (12). Heart rate, oxygen uptake, optical flow and accelerations of body segments were measured continuously. Subjects were instructed to refrain from caffeine intake and exercise three hours prior to testing.

Techniques

Pulmonary VO_2 and VCO_2 were measured by an automated on-line breath-by-breath system (Oxycon Pro, Jaeger, CareFusion, Hoechberg, Germany). Mean output values of 15 s. obtained at 2:45-3:45 of each exercise period were used for regression analysis.

of each exercise period to quantify the oxygen uptake at each speed. The volume transducer (Triple V) was calibrated using the internal flow generator (12 – 120 L $\cdot$ min^{-1}) and gas analysers were calibrated before and after each test using a calibration gas of known composition (O_2% =

15.10; CO_2% = 5.00%) and ambient air (O_2% = 20.93; CO_2% = 0.03%). Gross EE during each exercise period was calculated on the basis of (40). Calculation of net EE was done by subtracting estimated resting energy consumption (18) from gross EE.

Heart rate was recorded continuously with a RS800CX heart rate monitor (Polar Elektro Oy, Kempele, Finland).

Tri-axial accelerometry was used to quantify limb and torso (center of gravity) accelerations (wGT3X-BT, ActiGraph). Accelerometers were positioned at the subjects' right side. Accelerometer positions were proximal to the lateral malleolus (ankle), frontal between trochanter major and epicondyles lateralis (thigh), proximal to iliac crest (hip) and proximal to the styloid process (wrist). Accelerometers sampled at 80 Hz and vector magnitude accelerations were downloaded and calculated based on 10 s epochs using the Actigraph, ActiLife 6 software. Average accelerations (1g subtracted) obtained at min 2:50-3:50 of each exercise period were used for regression analysis. The time period for analysis was chosen in order to overlap with steady state oxygen uptake measurements.

Thermal imagery - Optical flow was measured using a thermal camera (AXIS Q1922, AXIS Communications, Sweden). Temperature sensitivity < 100 mK, with a sampling rate of 30 frames $\cdot s^{-1}$. The camera was placed 6 m from the treadmill and 1 m off the ground, facing the left side of the subject. Thermal cameras register thermal radiation from a person as pixel intensity. In registration of thermal flow only the position of the pixels constituting the subject in each frame is needed for calculation of optical flow. Due to automatic gain adjustment of the camera no ceiling effects exist within the physiological range. Furthermore, pixels, per se, are only used

for identification of the subject of interest. Noise related to electrical mains has not been reported (14) and therefore low pass filtering was not performed.

The analysis of optical flow relies on a second time derivative on a two-dimensional lattice topology of a squared region of interest, with a grid that spans only the person in the image. The algorithm is self-normalizing with camera resolution, distance and body size. The grid is specified by 60x60 pixels on the thermal image of 640x480 pixels. The differences in mean pixel position between frames and the frame rate generate the optical flow level. The movement of a subject's torso along the horizontal and vertical axis is referred in the following as global movement whereas movement of body segments (arm and leg movement) in relation to the torso is referred to as local movement. Optical flow measurements were calculated at min 2:45-3:45 of each exercise period. Furthermore, optical flow measurements were calculated at the beginning of each velocity in order to establish response time for valid optical flow measurements.

Camera detection of the person exposed for examination: To support background removal techniques and subsequent calculation of local movement, a histogram normalization of the video data, based on histogram data of the first frame, was performed. This approach enhances the quality of the video and gives a sharp contour of the subject. Because thermal imagery is based on the heat of objects, histogram normalization creates an equal starting position for different situations and conditions. Basing normalization on the first frame ensures similar conditions over time. Afterwards a threshold-based segmentation, improved with the help of morphology closing operation (33), was used to find the person in the image and create a binary mask (fig. 1A).

Estimation of Global Movement: To determine the global movement, a non-rigid object tracking was performed. The global movement of a person was defined as the movement of center of gravity. Because a stable center of gravity of a person in motion is hard to find, the center of gravity is approximated to be located in the chest of the person. This limits the tracking problem to a small area of the person's upper body. The tracking method used to determine the global movement is based on Speeded Up Robust Features (SURF) (2) with a Kanade-Lucas-Tomasi tracker (KLT) (31, 38). Displacement vectors of a non-rigid body produced by a KLT tracker are generally too diverse to estimate its global displacement. Limiting the tracking to the chest by using only SURF points of the upper body part produces more equal displacement vectors. To ensure that tracking points are not lost over time, the bidirectional error threshold is set to infinity. The bidirectional error measures the validity of displacement vectors by tracking the SURF points back and measuring the distance between their original position and the position found by backwards tracking. Ignoring invalid displacement vectors naturally produces outliers. To remove these as well as outliers produced by e.g. rapid hand movements a RANdom SAmple Consensus (RANSAC) (9) subset of displacement vectors is calculated. Finally the global movement between two frames is estimated by averaging the RANSAC subset of displacement vectors. For greater stability a threshold in the RANSAC procedure is used that prefers groups of vectors with small magnitudes. This helps the method picking the vector group of the actual body, as it is more likely to move slower than any other group coming from an arm or a leg. Additionally, errors can be corrected by looking at magnitude values of the global movement over a certain time frame.

Fig. 1B and 1C show the presented method for one frame and calculated values of one second (30 frames), respectively. It can be seen in fig. 1C that running on a treadmill produces a cyclic

movement in the vertical plane and an irregular movement in the horizontal plane. The movement in the vertical direction is an integrated part of walking and running and requires a large amount of energy that must be included to make correct estimations of activity. After calculating the global movement, the image sequence can be stabilized and cropped to a region of interest (ROI). This is done by a perspective translation and scaling resulting in a situation, where all motion is caused by local movement. This produces a similar situation to a laboratory setup, where a participant is running on a treadmill, as in accelerometer studies (for review see ref. 25) and it therefore becomes easy to verify our results with accelerations of the limbs. Due to the importance of the vertical direction, only the global horizontal movement is removed, while global vertical movements are not compensated.

Estimation of local movement: After stabilizing the scene the local motion can be determined and mapped to EE. To determine the movement of the body limbs the optical flow between two frames is calculated. Most current optical flow techniques are based on the energy minimization framework of Horn and Schunck (23) and the concept of coarse-to-fine image warping introduced by Lucas and Kanade (31), and perform a local optimization of down sampled images. The down sampling removes information and causes the flow not to be found, when the structures are smaller than their displacement. Descriptor matching in contrast is able to estimate large displacement vectors, but is lacking a geometric relationship and is only able to estimate a small number of correspondences. Furthermore, outliers are very likely. This dilemma has been described and addressed by Brox et al. (5) and extended by Brox and Malik (6). The resulting method is combining optical flow with descriptor matching being capable of calculating the Large Displacement Optical Flow (LDOF) for large and small structures. The method proposed (6) is used for calculating the optical flow of the body limbs. Due to the stabilization of the ROI

as well as noise in the input data and errors in the calculation of the LDOF values, not only flow caused by the person is detected. To compensate for this error all values in the LDOF results that lie outside the detected region of a person are set to zero. Fig. 1D shows two thermal images with overlaid amount of local movement of a person running and walking.

Estimating Energy Values: After calculating the optical flow values between frames, an $N \times M$ grid with a tile size of $s_x \times s_y$ pixels of mean values is created, eq. 1. The difference of the grid values between two frames i and $i-1$ represent a local change in flow (acceleration), eq. 2. The means of the magnitude accelerations between frame-sets eq. 3 express an energy value per frame.

$$v_{inm} = \sum_{x=ns_x}^{(n+1)s_x} \sum_{y=ms_y}^{(m+1)s_y} \frac{f_{xy}}{s_x s_y} \quad [1]$$

$$a_{inm} = \| v_{inm} - v_{(i-1)nm} \| \quad [2]$$

$$E_i = \sum_{n=0}^{N-1} \sum_{m=0}^{M-1} \frac{a_{inm}}{N\,M} \quad [3]$$

$$r = \max_{0 \le i < I} \frac{\sum mi}{X\,Y} \quad [4]$$

Where:

$i \in I$ is the i^{th} frame of I frames

$(x \in X, y \in Y)$ is the pixel position in an image with the dimensions (X,Y)

$(n \in N, m \in M)$ is a tile index of N x M tiles

(s_x, s_y) is the dimension of a tile

f_{xy} is the flow of a position (x, y)

v_{inm} is the mean velocity of tile (n,m) in frame i

a_{inm} is the mean magnitude acceleration of tile (n,m) in frame i

E_i is the estimated energy value of frame i

r is the ratio between body size and image dimensions

m_i is the binary mask of frame i

The resulting values resemble cyclic functions of different frequencies and amplitudes for corresponding walking and running speeds as demonstrated in fig. 2.

The grid acts hereby as a weighting function. Fine meshed grids support the influence of smaller body parts, while coarse-meshed grids suppress their influence as well as the influence of local errors in the LDOF calculation. This is caused by larger structures being less fragmented in coarse-meshed grids. The calculated results are not comparable as they are depending on the body size of the person as well as the size of the ROI and therefore they need to be normalized. With a standardized ROI comparable values can be achieved with compensating for the body size by multiplying the energy values with the factor r, eq. 4. The ratio r expresses the relation between the body size and the ROI. The cyclic movement of walking and running, as used in the example, should allow the estimation of oxygen uptake within a very short time period.

Data analysis and statistics: Data are presented as mean ± SEM, if not otherwise stated. For comparisons of mean values at different exercise intensities one-way analysis of variance (ANOVA) repeated measures was performed. Between and within subject variances are reported as mean sum of squares ($MS_{between}$ and MS_{within}, respectively). Post hoc comparisons were made using Bonferroni correction.

Linear regression analysis and Pearson's product-moment correlation (R) was used to assess the relationship between optical flow, oxygen uptake, energy expenditure, accelerations and running

speed. Pooled initial number of frames at all velocities for each subject (first frames at each velocity) required for optic flow measurements to reach consistency was analyzed for each subject.

P values below 0.05 were considered as significant in all analyses. All analyses were performed using statistical analysis software (IBM SPSS Statistics version 22.0, SPSS, Chicago, IL, USA).

RESULTS

All subjects completed all intervals from 3 to 16 km · h^{-1} , but 2 subjects failed to complete the 4 min interval at 18 km · h^{-1}. Data obtained during the final completed minute at 18 km · h^{-1} were used for these two subjects.

Mean heart rate, oxygen uptake, oxygen uptake in relation to body weight, gross and net energy expenditure increased with increasing treadmill velocities (Table 1). Increase in speed was linearly associated with oxygen uptake (R^2 = 0.93; P < 0.0001), oxygen uptake in relation to body weight (R^2 = 0.98; P < 0.0001), gross energy expenditure (R^2 = 0.97; P < 0.0001) and net energy expenditure (R^2 = 0.97; P < 0.0001). During running, heart rate on average increased with 10.1 -15.8 beats · min^{-1} with each exercise period and the lowest increase of 10.1 beats · min^{-1}occurred from 16.0 to 18.0 km · h^{-1}. Oxygen uptake on average increased with 332 – 516 ml O_2 · min^{-1} with each exercise period and the lowest increase of 332 ml O_2 · min^{-1} occurred from 8.0 to 10.0 km · h^{-1}, however, also a minor increase of 395 ml O_2 · min^{-1} occurred at the high velocities of 16.0 to 18.0 km · h^{-1}. Respiratory exchange ratio (RER) increased with higher walking and running speeds. During walking mean RER increased from 0.828 to 0.876 and during running RER continued to increase from 0.882 at 8 km · h^{-1}, reaching 1.062 at 18 km · h^{-1} (Table 1). Mean

RER values exceeded 1.0 when speed increased from 14.0 to 16.0 km · h^{-1}. Both gross and net EE increased with increasing speed (Table 1)

Mean vector magnitude accelerations are shown in fig. 3A-D. Highest values were obtained from the ankle and lowest from the hip. Wrist and thigh accelerometers showed similar values of vector magnitude accelerations. All mean vector magnitude accelerations increased with running speed and showed a strong linear relationship with oxygen uptake (fig. 3; $P < 0.0001$): wrist ($R^2 = 0.84$), hip ($R^2 = 0.85$), thigh ($R^2 = 0.93$) and ankle ($R^2 = 0.94$). Summarizing acceleration data from all four sites showed a strong correlation with optical flow ($R^2 = 0.93$; $P < 0.0001$).

The optical flow values also increased with increasing speed (Table 1). Although optical flow was not significantly different between 16 and 18 km · h^{-1}, a trend for increase in optical flow was apparent from 16 to 18 km · h^{-1}. The mean magnitude optical flow changes from a single subject observed through a 3 s period (90 frames) are presented in fig. 2.

Average values of optical flow for all 14 subjects demonstrated a strong correlation with oxygen uptake across all exercise intensities (Fig. 4; $R^2 = 0.96$; $P<0.0001$). Out of 126 observations, only two outliers were observed.

Number of frames necessary to assess a constant optical flow value reflecting walking and running speeds were examined using linear regression (Fig. 5). With the temporal resolution of 30 frames per s, less than 100 frames were required to give a valid calculation of the optical flow. Also, all individual R^2-values exceeded 0.9 and did not improve further by increasing number of frames.

DISCUSSION

The main finding in the present study is that EE during treadmill locomotion can be estimated fast and precisely (1-2 s. of processing per frame on a single tread) using thermal cameras without any need of mechanical or electronic equipment attached to the person observed. The process can be faster and close to real time using parallel computing.

Oxygen uptake and energy expenditure in relation to optical flow

Optical flow values demonstrated a strong correlation with gross oxygen uptake across all exercise intensities, and all individual associations also showed strong correlations (fig. 4). Optical flow was not significantly different between 16 and 18 km $\cdot$ h^{-1}. However, a trend for increase in optical flow was apparent from 16 to 18km $\cdot$ h^{-1}. This increase is substantiated by the confidence intervals (CI -0.169 to 0.719). As both VO_2 and accelerations at distal placed accelerometers increased with speed, it appears that the current methodology has limitations at higher running speed.

Energy expenditure values are gross values and resting EE was not measured during the lab session. Net EE was therefore estimated by subtracting standard resting EE (18) from gross EE (Table 1). Resting EE to gross EE is greater at lower exercise intensities (walking) compared with higher exercise intensities. Measuring actual resting EE would therefore have provided more precise net EE values.

Oxygen uptake and heart rate rose linearly with increasing walking and running velocities, as previously reported in studies examining indirect estimation of EE and accelerometry (4, 12). Even though heart rate is a valid indicator of EE, training status may influence the relationship between oxygen uptake and heart rate (20). Similarly, day-to-day variation in heart rate during

(28) and cardiac drift during exercise (19, 27) may also affect prediction of energy expenditure using heart rate measurements. With the present methodological approach only movements of body segments are evaluated and therefore the above-mentioned aspects of heart rate variation will not affect the estimation of EE.

Mean RER values for all subjects during the two final bouts (16 and 18 km · h^{-1}) exceeded 1.0 but did not reach 1.1 (Table 1), indicating an increase in anaerobic energy contribution. However, the individual increase in oxygen uptake was still significant between bouts, indicating that VO_2peak had not been reached by any subjects prior to the final 18 km · h^{-1} exercise bout. Excluding the values from the two subjects who did not complete the 18 km · h^{-1} bout from the analyses did not affect the relationship between oxygen uptake and optical flow.

Optical flow and accelerations of the limbs

In the present investigation optical flow was validated against oxygen uptake. As optical flow values primarily are generated through local movements (movement of limbs), accelerometer data was used to quantify limb movements of ankle, thigh and wrist and not for estimating energy consumption per se. Accelerations increased with higher speeds at all three limb positions verifying the linear relationship between ankle accelerations and speed as previously reported by Guinhouya and colleagues (15). These results suggest that optical flow, oxygen uptake and limb movements are closely related (fig. 3 and fig. 4), as also observed when ankle movements are related to activities of daily living (35). Furthermore, summarizing acceleration data from all four sites showed a strong correlation with optical flow (R^2 = 0.93; P < 0.0001), providing an additional criterion measure for the thermal imaging measure of energy expenditure. It is noteworthy that the change from walking to running resulted in an irregular increase in

accelerations, indicating that accelerometers positioned distally at the limbs may be imprecise in estimating EE when this transition occurs. Accelerations at the hip (~ center of gravity) also showed a linear increase with oxygen uptake and therefore confirm previous investigation where accelerations (collected from a force treadmill) increased up to 16 km · h^{-1} (24).

Response time for valid Optical flow measurements

Another main finding is the response time for quantifying EE using optical flow measurements. Fig. 5 shows that less than 100 frames are needed in order to get stable optical flow measurements across the speeds. Within 3-4 sec the optical flow thus reflects EE during walking and running. Traditionally, studies investigating steady state oxygen uptake have used exercise bouts of minimum 2-3 min during both walking (34) and running (11, 16) in order to establish steady state conditions. The method therefore provides a very low response time for quantifying aerobic EE of locomotion.

Perspectives and conclusions

While the design of the method allows free movement in space and any type of activity, a controlled setup was used during the tests to prove the concept and directly compare to known methodologies. The setup in the present study shows the potential of the method with constrained error sources. Hence, the optical flow measurements predict oxygen uptake and EE with high accuracy during horizontal treadmill walking and running. Even though this methodology provides a novel, non-invasive approach of measuring EE it has some limitations compared to well-established methods such as indirect calorimetry. The fractional rate of substrate utilization cannot be identified with the current methodology and therefore small differences in EE between subjects are not detected when moving at the same velocity.

Differences in walking and running economy may therefore be difficult to detect. The next step will be to estimate EE using optical flow with a single person performing specific movement patterns (e.g. walking, running) outside the laboratory. Additional future investigations should involve optical measurements during free-living activities, which will address challenges related to the camera angles with respect to the field and the direction of the person. One approach could be to combine two thermal cameras in order to estimate 3D motion (26) and then extract optical flow changes and correlate that with oxygen consumption obtained by a portable metabolic cart.

In conclusion, optical flow obtained using thermal imagery gives a precise estimation of the aerobic EE (oxygen uptake) during horizontal walking and running. Furthermore, the estimation is effective within 3-4 sec of a given walking or running velocity, which gives a very fast response time compared to a steady state oxygen uptake. The fact that the method requires no wearable devices enables new forms of investigation in the field of sports and movement research. In particular, this approach will make it more feasible to perform analyses of EE during exercise.

Acknowledgements

The authors thank the subjects for their time and effort in volunteering for this study. The authors also thank Dan Stieper Karbing, Ph.D. for valuable statistical support.

Conflict of Interest

The authors declare no conflicts of interest, financial or otherwise.

The results of the present study do not constitute endorsement by the American College of Sports Medicine.

References

1. Åstrand P-O. New Records in Human Power. *Nature*. 1955; 176:922-23.

2. Bay H, Tuytelaars T, Van Gool L. SURF: Speeded Up Robust Features. In: *Computer Vision ECCV 2006*: *Springer;* 2006, p. 404-417.

3. Brage S, Brage N, Franks PW, Ekelund U, Wareham NJ. Reliability and validity of the combined heart rate and movement sensor Actiheart. *Eur J Clin Nutr*. 2005; 59(4):561-70.

4. Brage S, Wedderkopp N, Franks PW, Andersen LB, Froberg K. Reexamination of validity and reliability of the CSA monitor in walking and running. *Med Sci Sports Exerc*. 2003; 35(8):1447-54.

5. Brox T, Bregler C, Malik J. Large displacement optical flow. In: *Proceedings of the Institute of Electrical and Electronics Computer Society Conference on Computer Vision and Pattern Recognition;* 2009 June 20-26: Miami, Fl, USA; 2009. p. 41-48.

6. Brox T, Malik J. Large displacement optical flow: descriptor matching in variational motion estimation. *IEEE Trans Pattern Anal Mach Intell*. 2011; 33(3):500-13.

7. Carter J, Jeukendrup AE. Validity and reliability of three commercially available breath-by-breath respiratory systems. *Eur J Appl Physiol*. 2002; 86(5):435-41.

8. Cavagna GA, Kaneko M. Mechanical work and efficiency in level walking and running. *J Physiol*. 1977; 268(2):467-81.

9. Fischler MA, Bolles RC. Random sample consensus:a paradigm for model fitting with applications to image analysis and automated cartography. *Communications of the ACM*. 1981; 24(6):381-95.

10. Foss O, Hallen J. Validity and stability of a computerized metabolic system with mixing chamber. *Int J Sports Med*. 2005; 26(7):569-75.

11. Franch J, Madsen K, Djurhuus MS, Pedersen PK. Improved running economy following intensified training correlates with reduced ventilatory demands. *Med Sci Sports Exerc*. 1998; 30(8):1250-6.

12. Fudge BW, Wilson J, Easton C, et al. Estimation of oxygen uptake during fast running using accelerometry and heart rate. *Med Sci Sports Exerc*. 2007; 39(1):192-8.

13. Fujiyoshi H, AJ Lipton. Real-time human motion analysis by image skeletonization. In: *Proceedings of the Institute of Electrical and Electronics Engineers Fourth Workshop on Applications of Computer Vision;* 1998 Oct 19-21: Princeton, NJ, USA. 1998. p. 15-21.

14. Gade R, Moeslund TB. Thermal cameras and applications: a survey. *Mach Vision Appl*. 2014; 25(1):245.

15. Guinhouya CB, Hubert H, Dupont G, Durocher A. Relationship Between the MTI Accelerometer (Actigraph) Counts and Running Speed During Continuous and Intermittent Exercise. *J Sports Sci Med*. 2005; 4(4):534-42.

16. Hagan RD, Strathman T, Strathman L, Gettman LR. Oxygen uptake and energy expenditure during horizontal treadmill running. *J Appl Physiol Respir Environ Exerc Physiol*. 1980; 49(4):571-5.

17. Han J, B Bhanu. Human activity recognition in thermal infrared imagery. In: *Proceedings of the Institute of Electrical and Electronics Engineers Computer Computer Society Conference Workshops on Computer Vision and Pattern Recognition;* 2005 June 25: San Diego, CA, USA. 2005 p. 17.

18. Harris JA, Benedict FG. A Biometric Study of Human Basal Metabolism. *Proc Natl Acad Sci U S A*. 1918; 4(12):370-3.

19. Heaps CL, Gonzalez-Alonso J, Coyle EF. Hypohydration causes cardiovascular drift without reducing blood volume. *Int J Sports Med*. 1994; 15(2):74-9.

20. Helgerud J, Hoydal K, Wang E, Karlsen T, Berg P, Bjerkaas M, Simonsen T, Helgesen C, Hjorth N, Bach R, Hoff J. Aerobic high-intensity intervals improve VO_2max more than moderate training. *Med Sci Sports Exerc*. 2007; 39(4):665-71.

21. Hill AV, Lupton H. The oxygen consumption during running. *J Physiol*. 1922; 56(suppl):xxxii–xxxiii.

22. Hongu N, Orr BJ, Roe DJ, Reed RG, Going SB. Global positioning system watches for estimating energy expenditure. *J Strength Cond Res*. 2013; 27(11):3216-20.

23. Horn BK, Schunck BG. Determining optical flow. In: Proceedings of the 25th Aniversary Conference of the International Society for Optical Engineering - *Technical Symposium East*; 1981 Nov: San Diego, CA, USA; 1981. p. 319-331.

24. John D, Miller R, Kozey-Keadle S, Caldwell G, Freedson P. Biomechanical examination of the 'plateau phenomenon' in ActiGraph vertical activity counts. *Physiol Meas*. 2012; 33(2):219-30.

25. Kozey SL, Lyden K, Howe CA, Staudenmayer JW, Freedson PS. Accelerometer output and MET values of common physical activities. *Med Sci Sports Exerc*. 2010; 42(9):1776-84.

26. Kristoffersen MS, Dueholm JV, Gade R, Moeslund TB. Pedestrian Counting with Occlusion Handling Using Stereo Thermal Cameras. *Sensors (Basel)*. 2016 [cited 2016 March 31];16(1). Available from: http://www.mdpi.com/1424-8220/16/1/62. doi: 10.3390/s16010062.

27. Lafrenz AJ, Wingo JE, Ganio MS, Cureton KJ. Effect of ambient temperature on cardiovascular drift and maximal oxygen uptake. *Med Sci Sports Exerc*. 2008; 40(6):1065-71.

28. Lamberts RP, Lambert MI. Day-to-day variation in heart rate at different levels of submaximal exertion: implications for monitoring training. *J Strength Cond Res*. 2009; 23(3):1005-10.

29. Liu S, Gao RX, Freedson PS. Computational methods for estimating energy expenditure in human physical activities. *Med Sci Sports Exerc*. 2012; 44(11):2138-46.

30. Livingstone MB, Prentice AM, Coward WA, et al. Simultaneous measurement of free-living energy expenditure by the doubly labeled water method and heart-rate monitoring. *Am J Clin Nutr*. 1990; 52(1):59-65.

31. Lucas BD, Kanade T. An iterative image registration technique with an application to stereo vision. In: *Proceedings of the seventh international joint conference on Artificial intelligence - Volume 2*.1981 Aug 24-28: Vancouver (Canada). University of British Columbia; 1981. p. 674-79.

32. Luke A, Maki KC, Barkey N, Cooper R, McGee D. Simultaneous monitoring of heart rate and motion to assess energy expenditure. *Med Sci Sports Exerc*. 1997; 29(1):144-8.

33. Moeslund TB. *Introduction to Video and Image Processing: Building real systems and applications*. Springer; 2012. 227 p.

34. Montoye HJ, Ayen T, Nagle F, Howley ET. The oxygen requirement for horizontal and grade walking on a motor-driven treadmill. *Med Sci Sports Exerc*. 1985; 17(6):640-5.

35. Parkka J, Ermes M, Antila K, van Gils M, Manttari A, Nieminen H. Estimating intensity of physical activity: a comparison of wearable accelerometer and gyro sensors and 3 sensor locations. In: *Proceedings of the 29th international conference of the Institute of Electrical and Electronics Engineers on Engineering in Medicine and Biology Society*. 2007 Aug 22-26: Lyon (France): 2007. p. 1511-4.

36. Poppe R. Vision-based human motion analysis: An overview. *Comput Vision Image Understanding*. 2007; 108(1-2):4 18.

37. Saltin B, Astrand PO. Maximal oxygen uptake in athletes. *J Appl Physiol*. 1967; 23(3):353-8.

38. Tomasi C, Kanade T. Detection and Tracking of Point Features. *Carnegie Mellon University Technical Report (CMU-CS).* 1991; 91-132.

39. Wang L, Hu W, Tan T. Recent developments in human motion analysis. *Pattern Recognit*. 2003; 36(3):585 601.

40. Weir JB. New methods for calculating metabolic rate with special reference to protein metabolism. *J Physiol*. 1949; 109(1-2):1-9.

FIGURE LEGENDS

FIGURE 1. A: Input frame and segmentation. B: SURF points (cross), RANSAC subset (circle) and scaled displacement vectors (line), which are used for estimating the global movement of a subject. C: The displacement per frame of the subset of feature points, marked in fig. 1B, in horizontal (X) and vertical (Y) direction. D: The optical flow between two frames augmented on the latter frame to visualize the actual optical flow registered.

FIGURE 2. Calculated mean magnitude flow change values for a subject covering one walking velocity (5.0 km · h^{-1}) and two different running speeds (8.0 and 18.0 km · h^{-1}).

FIGURE 3. Mean GT3X output (± SEM), plotted against relative oxygen uptake. GT3X outputs are sampled at A) wrist, B) hip, C) thigh and D) ankle.

FIGURE 4. Individual oxygen uptake measurements in relation to optical flow during walking (3-7 km · h^{-1}) and running (8-18 km · h^{-1}). Solid black regression line represents pooled data of all subjects (R^2 = 0.96; P<0.0001). Individual subject data are illustrated by different symbols

FIGURE 5. R^2 values plotted against the first numbers of thermal camera frames included in correlation analysis. Each line represents average values from one subject. 100 frames (3.33 s), marked by dashed vertical line indicate response time for quantifying aerobic energy expenditure by optical flow.

Figure 1

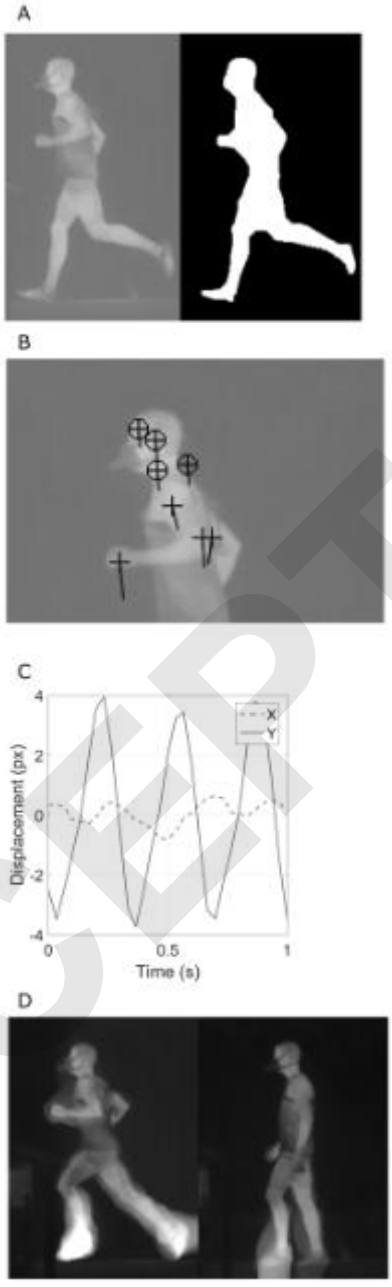

Figure 2

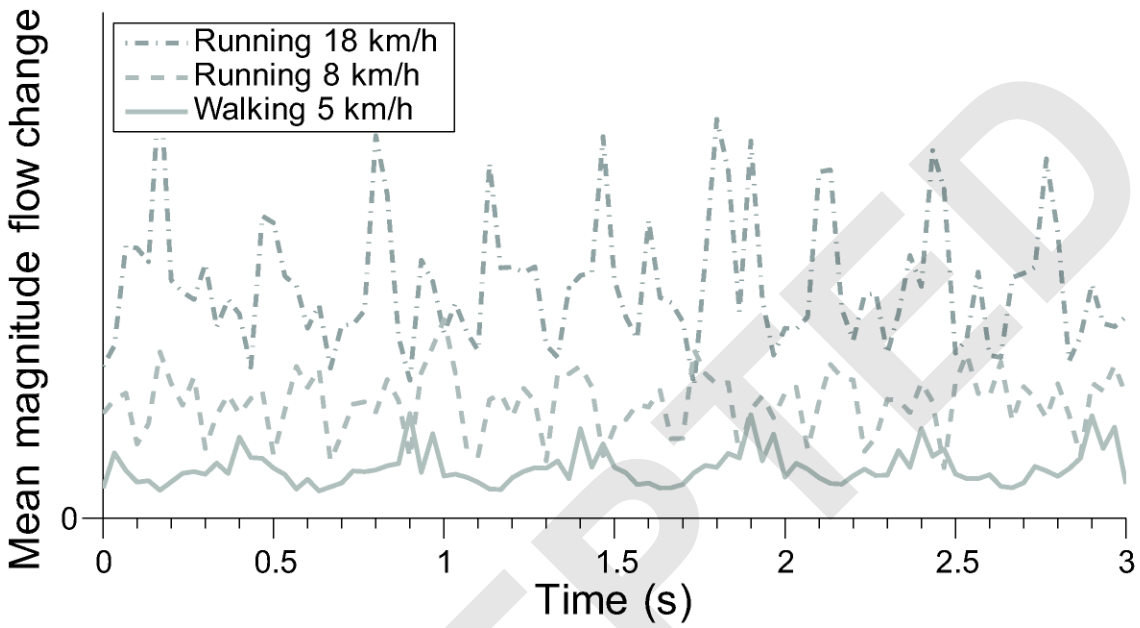

Figure 3

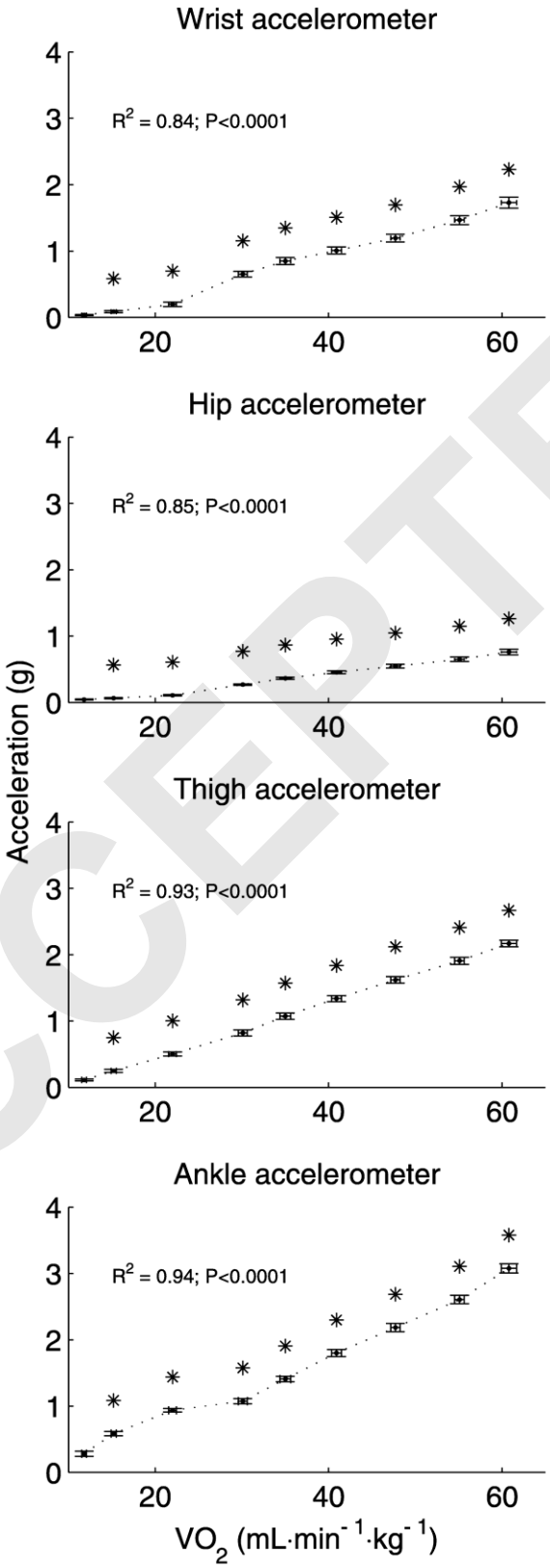

Figure 4

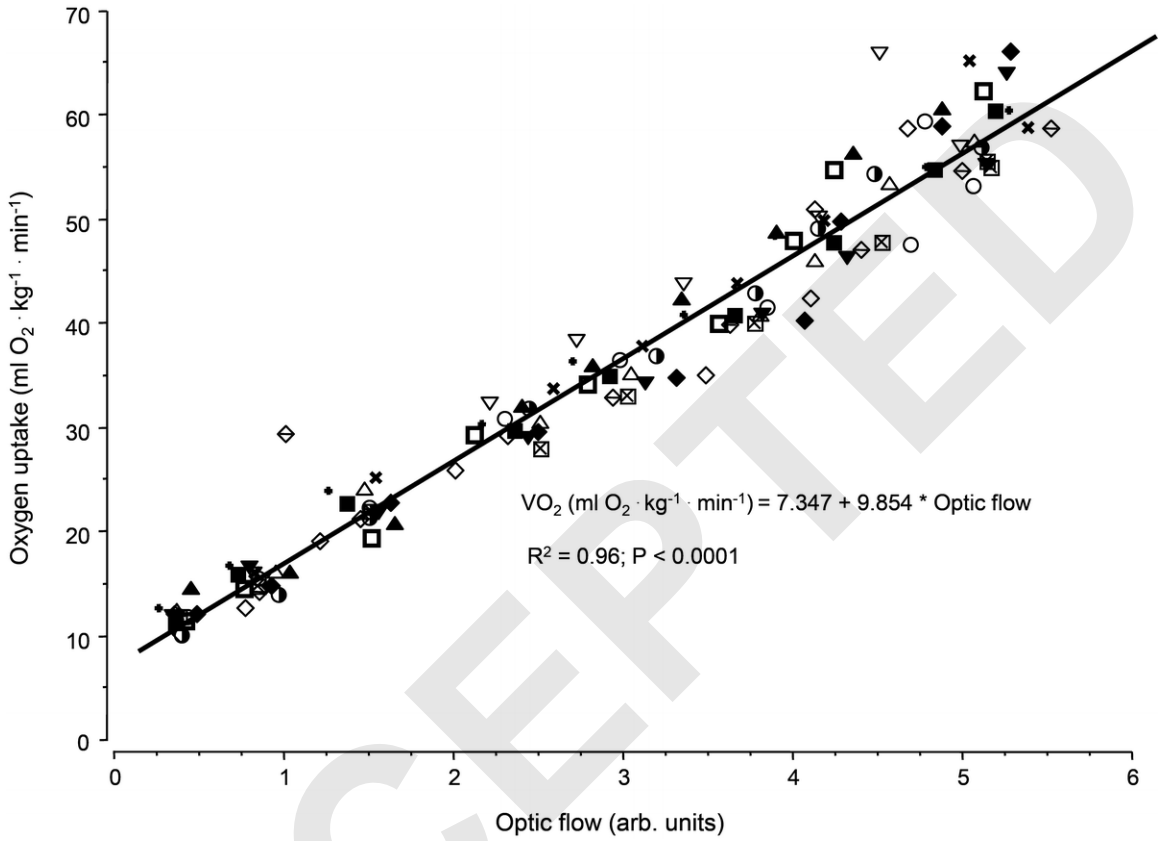

Figure 5

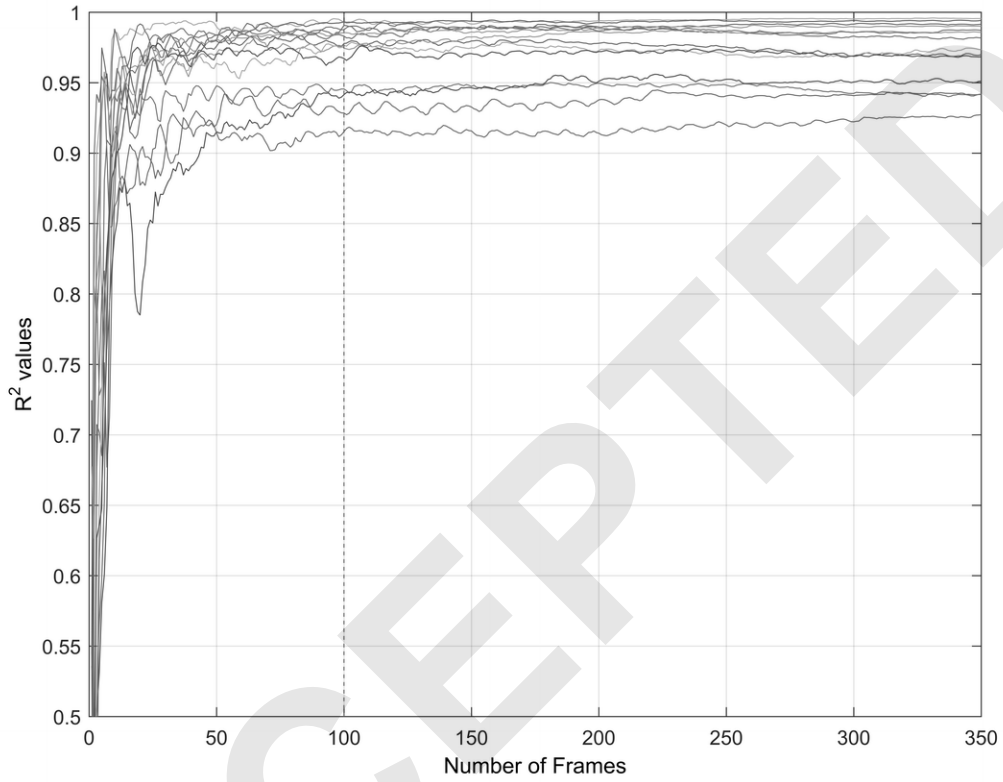

TABLE 1: Heart rate, oxygen uptake, RER-values, energy expenditure and optical flow (mean±SE) at increasing treadmill velocities. ANOVA variance between and within subjects is expressed as mean sum of squares ($MS_{between}$ and MS_{within}, respectively). $^{\alpha}$n = 13. * Significantly different from previous value ($p<0.05$).

	Walking			**Running**						
	Treadmill velocity ($km \cdot h^{-1}$)			**Treadmill velocity ($km \cdot h^{-1}$)**						***ANOVA***
	3.0	**5.0**	**7.0**	**8.0**	**10.0**	**12.0**	**14.0**	**16.0**	**18.0**	$MS_{betweem}$ MS_{within}
Heart rate$^{\alpha}$ (bpm)	**74.3 ±2.8**	**82.8* ±3.1**	**97* ±3.4**	**116.5* ±3.7**	**128.5* ±4.3**	**144.3* ±4.9**	**158.0* ±4.4**	**171.7* ±3.7**	**181.8* ±3.8**	***1397 15389***
Gross Oxygen uptake ($L\ O_2 \cdot min^{-1}$)	**0.82 ±0.03**	**1.06* ±0.03**	**1.53* ±0.05**	**2.11* ±0.08**	**2.44* ±0.09**	**2.86* ±0.10**	**3.33* ±0.10**	**3.85* ±0.11**	**4.24* ±0.12**	***0.68 1.53***
Gross Oxygen uptake ($ml\ O_2 \cdot kg^{-1} \cdot min^{-1}$)	**11.79 ±0.27**	**15.21* ±0.29**	**21.96* ±0.44**	**30.14* ±0.52**	**34.94* ±0.62**	**40.87* ±0.57**	**47.73* ±0.53**	**55.14* ±0.56**	**61.21* ±0.87**	***20.6 155.2***
RER	**0.83 ±0.02**	**0.84 ±0.01**	**0.88 ±0.02**	**0.88 ±0.01**	**0.91* ±0.01**	**0.92 ±0.02**	**0.95* ±0.02**	**1.01* ±0.02**	**1.06* ±0.01**	***0.02 0.03***
Gross energy expenditure ($J \cdot kg^{-1} \cdot min^{-1}$)	**237.4 ±5.3**	**307.1* ±5.4**	**449.2* ±8.9**	**616.8* ±10.3**	**726.0* ±12.9**	**849.1* ±11.7**	**995.6* ±12.2**	**1165.2* ±12.7**	**1300.4* ±17.0**	***8339 69910***
Net energy expenditure ($J \cdot kg^{-1} \cdot min^{-1}$)	**165.7 ±5.4**	**235.5* ±5.5**	**377.6* ±9.2**	**545.1* ±10.7**	**654.4* ±13.1**	**777.5* ±11.9**	**923.9* ±12.2**	**1093.6* ±12.5**	**1228.8* ±17.3**	***8417 69906***
Optic flow (arb. units)	**0.39 ±0.01**	**0.85* ±0.03**	**1.48* ±0.03**	**2.26* ±0.11**	**2.93* ±0.07**	**3.66* ±0.06**	**4.21* ±0.060**	**4.79* ±0.10**	**5.06 ±0.07**	***0.16 1.60***